Cancer Chemother Pharmacol (2012) 69:185–194
DOI 10.1007/s00280-011-1684-y

ORIGINAL ARTICLE

Evaluating rational non-cross-resistant combination therapy in advanced clear cell renal cell carcinoma: combined mTOR and AKT inhibitor therapy

William S. Holland · Clifford G. Tepper · Jose E. Pietri · Danielle C. Chinn · David R. Gandara · Philip C. Mack · Primo N. Lara Jr.

Received: 7 December 2010 / Accepted: 22 May 2011 / Published online: 5 June 2011

Abstract
Purpose Inhibition of the mammalian target of rapamycin (mTOR), a regulator of hypoxia inducible factor (HIF), is an established therapy for advanced renal cell cancer (RCC). Inhibition of mTOR results in compensatory AKT activation, a likely resistance mechanism. We evaluated whether addition of the Akt inhibitor perifosine to the mTOR inhibitor rapamycin would synergistically inhibit RCC.
Methods Select RCC cell lines were studied [786-O, A498 (VHL mutant), CAKI-1 (VHL wild type), and 769-P (VHL methylated)] with single agent and combination therapy. Growth inhibition was assessed by MTT and cell cycling by flow cytometry. Phospho-AKT (S473) and HIF-2α were assessed by Western blot. Total RNA was isolated from 786-O cells subjected to single agent and combination treatments. In these cells, genome-wide expression profiles were assessed, and real-time PCR was used to confirm a limited set of expression results.
Results Three out of four cell lines (CAKI-1, 769-P, and 786-O) were sensitive to single-agent perifosine with 50% inhibitory concentrations ranging from 5 to 10 μM. Perifosine blocked phosphorylation of AKT induced by rapamycin and inhibited HIF-2α expression in 786-O and CAKI-1. Combined treatment resulted in sub-additive growth inhibition. GeneChip analysis and pathway modeling revealed inhibition of the IL-8 pathway by these agents, concomitant with up-regulation of the KLF2 gene, a known suppressor of HIF1α.
Conclusions Perifosine is active in select RCC lines, abrogating the induction of AKT phosphorylation mediated by mTOR inhibition. Combined mTOR and AKT inhibition resulted in the modulation of pro-angiogenesis pathways, providing a basis for future investigations.

Keywords mTOR · AKT · Perifosine · Rapamycin · Renal cell cancer

Introduction

The mammalian target of rapamycin (mTOR) is a serine/threonine kinase that recognizes stress signals via the PI3K-AKT pathway and phosphorylates p70 ribosomal S6 kinase 1 (S6K1) and eukaryotic initiation factor 4E binding protein 1 (4EP1). The mTOR pathway is a known regulator of hypoxia inducible factor (HIF), an essential driver of clear cell renal cell cancer (RCC) largely due to disruption of the von Hippel Lindau (vHL) tumor suppressor gene. Two large randomized phase III clinical trials have established the role of mTOR inhibition (with the agents temsirolimus and everolimus) as a sound therapeutic strategy in advanced RCC. In the first trial, temsirolimus was shown to significantly improve survival in a select population of RCC patients with poor-risk features [1]. Patients who received temsirolimus alone had longer survival (HR for death = 0.73; 95% CI: 0.58–0.92; $P = 0.008$) than patients who received IFN alone. In the second trial, everolimus was evaluated in a placebo-

Electronic supplementary material The online version of this article (doi:10.1007/s00280-011-1684-y) contains supplementary material, which is available to authorized users.

W. S. Holland · C. G. Tepper · J. E. Pietri · D. C. Chinn · D. R. Gandara · P. C. Mack (✉) · P. N. Lara Jr.
University of California, Davis Cancer Center,
4501 X Street, Suite, 3016, Sacramento, CA 95817, USA
e-mail: pcmack@ucdavis.edu

P. N. Lara Jr.
The VA Northern California Health Care System,
Mather Field, CA, USA

controlled phase III study in RCC patients who had failed prior therapy with VEGFR-TKIs [2]. In this heavily pretreated cohort, median PFS was significantly improved from 1.9 months (95% CI: 1.8–1.9) in the placebo arm to 4.0 months (95% CI: 3.7–5.5) in the everolimus arm (HR = 0.30; 95% CI: 0.22–0.40; $P < 0.0001$). As a result of these randomized trials, both temsirolimus and everolimus have since been US Food and Drug Administration-approved for advanced RCC therapy.

Although these trials have validated the activity of single-agent mTOR inhibitors in RCC, efforts to optimize their efficacy by combining them with other therapeutic agents active against RCC have thus far been unsuccessful. In part, the failure of this strategy is due to the undue haste by investigators in empirically testing combination regimens in the clinic prior to adequate preclinical testing. For example, the combination of temsirolimus with interferon proved no better than single-agent temsirolimus in the phase III setting [1]. Furthermore, the empiric combination of temsirolimus plus the angiogenesis inhibitor sunitinib has not been found to be feasible in a phase I study due to unacceptable toxicity [3]. Although a phase II trial of everolimus in combination with the anti-VEGF monoclonal antibody bevacizumab demonstrated feasibility of this approach, a subsequent randomized phase II trial (the TORAVA trial) suggested that this doublet performed no better than already approved standard therapies such as single-agent sunitinib or bevacizumab + interferon [4, 5].

In view of these challenges, we sought to preclinically explore ways to optimize mTOR inhibitor-based combination therapy. Specifically, we pursued a strategy in which mTOR inhibition was assessed in the context of Akt inhibitor therapy in clear cell RCC. Since it had become clear that one potential resistance mechanism to single agent mTOR inhibitor therapy was feedback activation of the Akt pathway, we hypothesized that the combination of rapamycin and perifosine, an orally bioavailable Akt inhibitor, would result in abrogation of the Akt feedback loop and thus result in synergistic activity against RCC [6–10].

Methods

Cell culture and reagents

The kidney cell lines CAKI-1, 786-O, 769-P, and A498 were purchased from American Type Culture Collection (Manassas, VA). All cell lines were maintained in RPMI supplemented with 10% FBS (JR Scientific, Woodland, CA), 1X Penicillin/Streptomycin/L-Glutamine, and 1X MEM vitamin solution (Invitrogen, Carlsbad, CA). Perifosine was provided by Keryx Biopharmaceuticals (New York, NY). Stock solutions of 100 mM were made in 100% EtOH. Rapamycin was obtained from Sigma–Aldrich (St. Louis, MO). Stock solutions of 1 mM were made in 100% EtOH.

Proliferation assay

Cell lines were plated at 1,500–2,000 cells/well in 96-well plates or 35-mm dishes in the presence of media and were allowed to attach overnight prior to treatment. Plating density was determined through growth curves analyzing doubling time of each cell line. All experiments were repeated at least 3 times. Cells were treated with single-agent perifosine (at concentrations ranging from 0.5 to 40 μM) or rapamycin (at concentrations ranging from 0.5 to 1,000 nM) or a combination of perifosine and rapamycin (at concentrations of 1.25–20 μM or nM, respectively). MTT (3-[4,5-dimethylthiazol-2-yl]-2,5-diphenyltetrazolium bromide; Thiazolyl blue) (Sigma, St. Louis, MA) assays were performed as previously described to assess growth following 3 days of treatment [11]. For longer-term proliferation assays, cells were treated for 72h with perifosine and/or rapamycin in 35-mm dishes, after which they were grown in drug-free media for an additional 5 days. Cells were fixed with glutaraldehyde (Fisher Scientific, Suwanee, GA) and stained with crystal violet (Fisher Scientific, Suwanee, GA) as described by Franken et al. or treated with MTT [12].

Immunoblot analysis

Protein extracts were prepared from cell pellets using *RIPA buffer* (*150 mM NaCl, 10 mM Tris–HCl, pH 8.0, 5 mM EDTA, 1% TritonX-100* (*Sigma*)) *containing 10 mg/ml leupeptin, 0.1 M aprotinin, 0.1 M PMSF, and 0.1 M* $NaVO_4$ (*Sigma*) as previously described [11]. Following extraction, protein samples were stored at −80°C prior to use. Protein concentration was determined using the BCA Protein Assay Reagent (Pierce, Rockford, IL). Proteins were separated on 12–15% SDS–PAGE mini gels and transferred to nitrocellulose membranes. Membranes were blocked using 2% Blotting Grade Blocker Non-Fat Dry Milk (Bio-Rad, Hercules, Ca) and then probed with specific antibodies including pAKT (s473), total AKT (Cell Signaling Technology), HIF2α (Novus), PARP (Santa Cruz Biotechnology), and β-actin (Sigma) according to the manufacturers specifications. After washing with TBST, membranes were incubated with a horseradish peroxidase-linked anti-mouse or anti-rabbit secondary antibody (1:5,000 dilution) (Promega, Madison, WI), washed again, and then incubated with enhanced chemiluminescence reagent (Amersham-Pharmacia, Piscataway, NJ). Labeling is detected using X-ray film (Kodak, Rochester, NY). Images were scanned using an HP ScanJet 6300C (Hewlett Packard, Houston, TX).

Flow cytometry

Cells (7.5×10^5 cells) were seeded into 100-mm dishes and allowed to adhere overnight. Cells were then treated with Perifosine, Rapamycin, or a combination of both. At 24 and 72 h post-treatment, cells were harvested by trypsinization and prepared for cell cycle analysis as previously described [13]. Cells were re-suspended in 0.5 ml PBS (pH7.4) then fixed in a final concentration of 70% ethanol and stored at −20°C. Prior to analysis, cells were washed once with PBS (pH7.4) and re-suspended in 0.9 ml PBS (pH7.4) with 5 µl of DNase-free RNase (Fermentas, Hanover, MD) then incubated at 37°C for 30 min. Propidium iodide (Boehringer Mannheim Corp., Indianapolis, IN) was added to a final concentration of 50 µg/ml, and samples are allowed to stand at room temperature, protected from light, for 10 min. DNA content/cell number was measured by assessing propidium iodide fluorescence using a Becton–Dickinson FACScan Flow Cytometer (Beckman Coulter, Miami, FL), while data analysis was conducted using CellQuest Software. Cells (5×10^4) were analyzed per experimental group, and all experiments were repeated three times.

Microarray gene expression profiling

786-O renal carcinoma cells were treated with rapamycin or perifosine as single agent or in combination. Total RNA was extracted using the RNeasy mini kit (Qiagen, Valencia, Ca), and RNA integrity evaluated by analysis with the Agilent 2100 Bioanalyzer (Agilent Technologies). Microarray analysis was performed by the UC Davis Cancer Center Genomics and Expression Resource. Genome-wide expression profiling using Human Genome U133 Plus 2.0 GeneChip arrays (HG-U133 Plus 2.0; Affymetrix, South San Francisco, CA) was performed according to the manufacturer's protocols and as previously described [14]. Data analysis was performed with the GeneSpring GX (version 11) software suite (Agilent Technologies, Santa Clara, CA). Briefly, robust multiarray average (RMA) [15] was used for probe summarization and normalization of background-adjusted, normalized, and log-transformed perfect match (PM) probe intensity values from the Cel raw data files. Comparison analysis was then performed in order to identify genes that were differentially expressed in the different treatment groups, and unbiased hierarchical clustering performed in order to identify co-expression clusters that were distinctive for each treatment group. Criteria for the selection of genes exhibiting significant expression changes included an average fold change of ≥ 1.75 between groups and P values of ≤ 0.05. Potential functions and pathways affected by the treatments were queried by organizing the genes based upon gene ontology (GO) annotations for biological process and molecular function and by conducting Gene Set Enrichment Analysis (GSEA) using the C2-C4 collections of gene sets in the Molecular Signatures Database (MSigDB) [16]. Additional pathway analysis and network visualization of the differentially expressed genes were then performed with Ingenuity Pathway Analysis (Ingenuity Systems, Inc.).

Real-time quantitative PCR

Total RNA was extracted from cells using the RNeasy mini kit (Qiagen, Valencia, Ca) following manufacturer's instructions. cDNA was synthesized from 500 ng of total RNA using the SuperScript® III First-Strand Synthesis System for RT–PCR (Invitrogen). Real-time PCR was conducted using the SYBR® GreenER™ qPCR SuperMix (Invitrogen) and an iQ5 Real-Time PCR detection system (BioRad, Hercules, Ca) for IL-8 (Genbank accession no. NM_000584), KLF2 (Genbank accession no. NM_016 270), VEGFA (Genbank accession no. NM_001025370), and β-actin (Genbank accession no. NM_001101). Primers were as follows: IL-8 (forward, 5′-ATG ACT TCC AAG CTG GCC GTG GCT-3′; reverse, 5′-TCT CAG CCC TCT TCA AAA ACT TCT C-3′) [17], KLF2 (forward, 5′-TGC GGC AAG ACC TAC ACC AAG AGT-3′; reverse, 5′-AGC CGC AGC CGT CCC AGT T-3′) [18], VEGFA (forward, 5′- TAC CTC CAC CAT GCC AAG TG-3′; reverse, 5′- ATG ATT CTG CCC TCC TCC TTC-3′) [19], β-actin (forward, 5′- GAG CGC GGC TAC AGC TT-3'; reverse, 5′-Reverse: TCC TTA ATG TCA CGC ACG ATT T-3′). PCR conditions, including primer concentration and annealing temperature, were optimized for each amplicon. A melt curve was included following all PCR reactions to ensure minimal amount of artifact formation. A standard curve was generated for each target-specific amplicon using six 5-fold dilutions of cDNA from universal RNA (Stratagene, Cedar Creek, Tx), and the efficiency of each RT–PCR reaction was determined. β-actin was used as a reference gene for all assays. The software package Q-Gene [20, 21] was used to determine the mean normalized expression (MNE) for each gene.

ELISA

Cells were seeded at a concentration of 5,000 cells/dish into 35-mm dishes and allowed to adhere overnight. Cells were then treated with Perifosine, Rapamycin, or a combination of both. At 72 h post-treatment, the supernatant was removed, briefly centrifuged, and stored at −20°C. All treatments were repeated twice with a minimum of two replicates per trial. An ELISA was performed using the Quantikine Human VEGF kit (R&D systems, Minneapolis, MN) following manufacturer's protocol. The optical density was determined using a microplate reader set to

450 nM with a wavelength correction of 570 nM. The concentration of VEGF was determined relative to a standard curve.

Statistical analysis

For the combination studies, we calculated the expected or theoretical inhibition of combined treatment with perifosine and rapamycin using the Bliss independence model as previously described [22]. Briefly, we used the equation $E_{\text{Bliss}} = E_{\text{A}} + E_{\text{B}} - E_{\text{A}} \times E_{\text{B}}$, where E_{A} and E_{B} are the fractional inhibitions of drug A (perifosine) or drug B (rapamycin) at specific concentrations to derive a theoretical value of combined inhibition if both agents acted independently of each other to inhibit growth. All plots were generated using GraphPad Prism 5 version 5.03 for Windows (GraphPad Software, San Diego California USA, www.graphpad.com).

Results

Perifosine inhibits pAKT and proliferation in RCC cell lines

Four RCC cell lines were assessed for sensitivity to perifosine: 786-O, CAKI-1, 769-P, and A498. Of these, only CAKI-1 has a functional vHL protein (see Table 1). All of the RCC cell lines showed a dose-dependent decrease in proliferation although the magnitude and potency of the inhibition varied. Three of the four RCC cell lines (786-O, CAKI-1, and 769-P) showed a moderate sensitivity to perifosine, with IC50s between 5–10 μM (Fig. 1). These are within the clinically achievable peak plasma concentrations for perifosine that have been reported in patients in the range of 12–15 μM [8, 23]. A498 cells were largely insensitive, not having reached an IC50 even at high doses of perifosine (40 μM).

Following treatment with perifosine, we observed a dose-dependent inhibition of pAKT (S473) levels in 786-O (Fig. 2a). This reduction also coincided with a partial inhibition of pMAPK (p44/42). As 5 μM perifosine was sufficient to abolish >80% of pAKT (S473) levels by 24 h, we next conducted a time-course experiment to examine the effects on pAKT (S473) over time. As shown, by 3 h of treatment, a reduction in pAKT (S473) levels was observed that was sustained through 72 h of treatment in both the 786-O (Fig. 2b) and CAKI-1 (Fig. 2c) cell lines. There were no observable changes in total AKT levels following treatment in contrast to other published reports with perifosine [24]. In both the vHL wt (CAKI-1) and vHL-mutant (786-O) cell lines, an initial increase in HIF2alpha expression was observed up to 24h followed by a reduction to baseline or lower levels by 72h. We also observed increased cleavage in PARP at 24h indicating some cytotoxicity from the single-agent treatment.

Perifosine abrogates rapamycin-induced pAKT

The four RCC cell lines were also tested with the combination of perifosine and the mTOR inhibitor rapamycin. For each cell line, a plateau in growth inhibition at low (5–10 nM) doses was observed prior to or just after reaching an IC50 (data not shown). Previous reports have indicated that these concentrations are sufficient to inhibit mTOR and its downstream targets [6]. Drug combination interactions were originally designed for median-effect analysis as described by Chou and Talalay [25]. Using a constant combination ratio, the cell line panel was treated with a twofold serial dilution (4X, 2X, 1X, 0.5X, and 0.25X where X would represent an effective median dose) of each drug as a single agent or in combination for 72h after which cellular proliferation was measured by MTT (Fig. 3a–d). For this study, the defined median dose for perifosine was 5 μM, while 5 nM was considered the median dose for rapamycin. As combination index or isobologram analysis necessitate an established ED50 or IC50 dose that was not always observable in the single-agent dose-response curves, the Bliss independence model for additivity was used. Under this model, both perifosine and rapamycin are assumed to act in a nonexclusive or independent manner on one or more targets/pathways. To observe additivity from a combination treatment, the fractional response of both agents in combination must be equal to the sum of the two fractional responses minus their product. One of the benefits of the Bliss model is that it may evaluate changes in both potency (e.g., IC50 dose) and maximal efficacy. As shown for all cell lines, the observed inhibition in the combination was generally lower than what would be expected if each agent were acting independently (as

Table 1 RCC cell line panel and characteristics

Cell Line	Histology	VHL	p53	PTEN
786-O	Clear cell	311delG	832C > G	445C > T
A498	Clear cell	426_429delTGAC	Wt	Wt
769-P	Clear cell	Methylated	Wt	Wt
CAKI-1	Clear cell	Wt	Wt	Wt

All mutations have been confirmed by direct sequencing

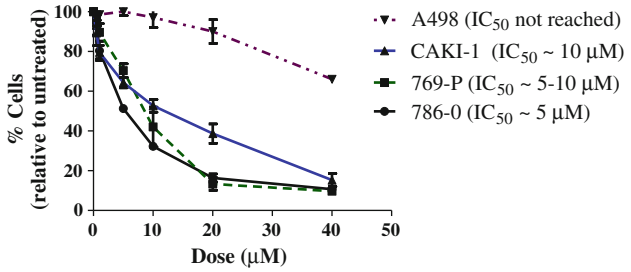

Fig. 1 Growth curves of single-agent perifosine in RCC cell lines. Cells were treated 3 days prior to MTT. Legend is in the order of sensitivity

derived from the Bliss model). However, this difference was minimal in the 769-P and CAKI-1 (approximately 2.6 and 6.3%, respectively). In 786-O, the combined effect was similar to that of perifosine alone, approximately 12.6% below the Bliss estimate. At the molecular level, the combination treatment was sufficient to abrogate the rapamycin-induced increase in pAKT expression in the 786-O cell line despite showing no additivity (Fig. 3e).

Cell cycling analysis of single agent and combination with rapamycin

To determine the cell cycle response to perifosine and rapamycin, as single agents and in combination, flow cytometric analysis of DNA content was used. The CAKI-1 and 786-O cell lines were selected for further study. Each cell line was treated with 5 μM perifosine and/or 10 nM rapamycin for 24- and 72h prior to being harvested. In both cases, the observed changes in DNA content were much broader and more prolonged in the CAKI-1 cell line compared to the 786-O (Fig. 4). After 72h, perifosine primarily resulted in an accumulation of G2/M DNA content (an absolute increase of 8.38 and 33.12%, for 786-O and CAKI-1, respectively, compared to untreated) with a reduction in G0/G1 (−0.45 and −22.21%) and S-Phase (−7.93 and −10.89%). In contrast, single-agent rapamycin resulted in increased G0/G1 content (13.15 and 17.84%) concurrent with a decreased S-Phase (−9.10 and −12.33%) and G2/M (−3.33 and −5.50%). Combination treatment with perifosine and rapamycin produced varied results in each of the cell lines. For the 786-O cells, after 72h, the combination treatment resulted in an increase in G0G1 (9.35%) and G2/M (2.80%) content with a reduction in S-Phase (−12.14%). The CAKI-1 cells on the other hand continued to show a strong increase in G2/M (24.90%) with a reduction in G0G1 (−14.08%) and S-Phase (−10.81%). Notably, the effects observed on the cell cycle following combination treatment were not as pronounced as the changes seen following single-agent treatment. This trend was also observed in the sub-G1 content where single agent had slightly greater sub-G1 accumulation than the combination treatment (6.49 vs. 2.41% and 7.25 vs. 5.20% in 786-O and CAKI-1, respectively). Rapamycin-dependent effects appeared to be more dominant in the 786-O cells following combination treatment. These results were confirmed by a long-term growth assay demonstrating minimal enhancement in the combination compared to perifosine alone (see Online Resource 1).

Gene expression analysis of single-agent perifosine and combination with rapamycin

A genome-wide expression profile was performed on the 786-O (vHL mutant) cell line following treatment with perifosine and/or rapamycin. As RCC is a heavily vascularized disease, its development and subsequent metastasis requires an array of pro-survival and pro-angiogenic factors that may also contribute to drug resistance. While the combination treatment did not enhance the cytotoxicity or anti-proliferative activity of the single agents in vitro, significant changes in the transcriptional program for RCC may still occur. Gene expression analysis was performed on two independent treatment replicates using the Affymetrix HG-U133 Plus 2.0 array, a GeneChip-based microarray that allows for the analysis of more than 47,000 transcripts. Filtering for selected genes was done as described in the methods, with a fold change of 1.75 or

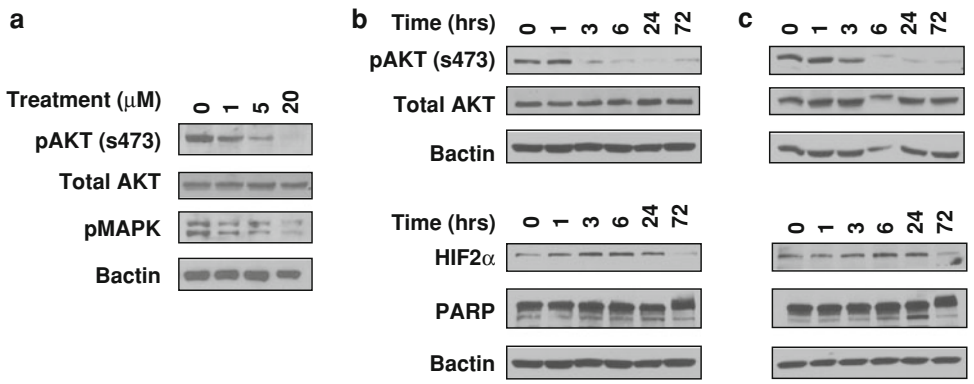

Fig. 2 **a** Dose response of perifosine in 786-O. Cells were treated with single-agent perifosine at indicated doses and harvested at 24 h. Time courses following perifosine treatment in (**b**) 786-O (VHL mutant) and (**c**) CAKI-1 (VHL wt). Cells were treated with 5 mM perifosine and harvested at indicated time points

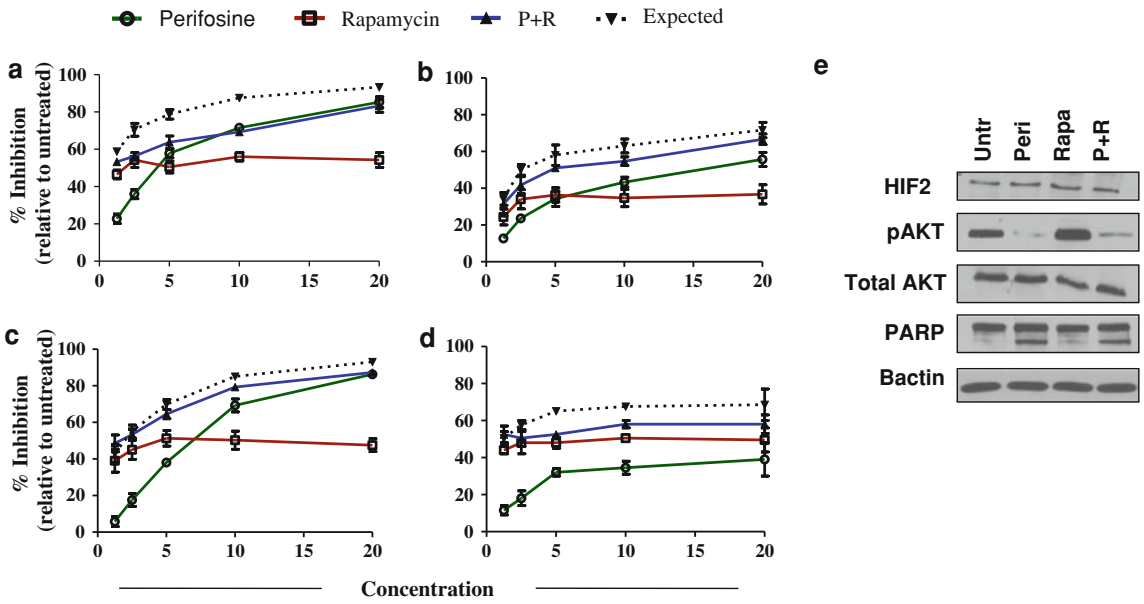

Fig. 3 Growth curves of RCC cell lines (**a**) 786-O, (**b**) CAKI-1, (**c**) 769-P, and (**d**) A498 following 72 h of treatment with single-agent perifosine (mM), rapamycin (nM), or the combination. Data are graphed as % inhibition relative to untreated cells. The expected line is derived from the Bliss independence model and represents the expected inhibition of the combination if it showed additivity. **e** Protein expression of pAKT(S473) following treatment with perifosine (5 mM), rapamycin (10 nM), and the combination for 24 h in 786-O cells

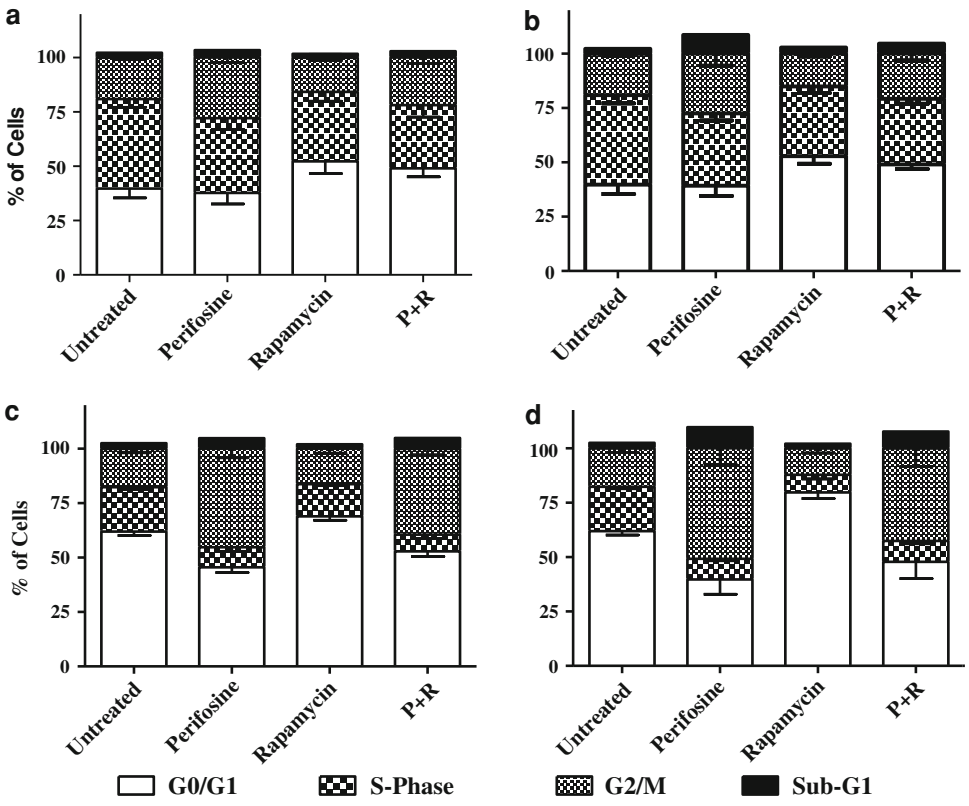

Fig. 4 Flow cytometric analysis of DNA content in the RCC cell lines 786-O and CAKI-1. Cells were treated with 5 mM perifosine and/or 10 nM rapamycin. Graphed are the results for 786-O cells treated for (**a**) 24 h and (**b**) 72 h and CAKI-1 cells treated for (**c**) 24 h and (**d**) 72 h. SubG1 content is represented in the *upper component* of each *graph*

greater and P values of ≤ 0.05. Single-agent treatment of perifosine resulted in 46 genes with a twofold or greater change in expression with 17 and 29 having higher or lower expression, respectively. Rapamycin treatment resulted in 94 genes with a twofold or greater change in expression, of which 72 showed higher expression and 22

were identified with lower expression. A total of 305 genes were found to be differentially expressed by twofold or more in the combination treatment with 194 genes being highly expressed, and 111 genes having reduced expression. As shown by the heat map in Fig. 5a, the combination treatment generally showed more differential expression than either single-agent treatment alone, suggesting an increase in transcriptional regulation following treatment with both agents. Of the genes exhibiting twofold or greater changes in expression, only 53 (27.3%) of the 194 genes with higher expression in the combination also had higher expression following perifosine and/or rapamycin single-agent treatment. Of the 111 genes with lower expression (≥2-fold change) in the combination, only 20 (18%) also had lower expression in either or both of the single-agent treatments. A divergent expression pattern was observed in a small subset of genes in the combination compared to the single-agent treatments, where changes in the combination, relative to the untreated control, were apparently minimized. For single-agent perifosine, 5 (29.4%) of the most highly expressed genes (≥2-fold change) and 19 (65.5%) of the lower expressed genes (≥2-fold change) showed a reduction in the fold change in the combination. For rapamycin 26 (36%) of the highly expressed genes (≥2-fold change) and 7 (31.8%) of the lower expressed genes (≥2-fold change) showed a reduction in the fold change in the combination.

qRT–PCR validation of selected genes

Among the genes that showed the greatest differential changes in expression were the transcription factor Kruppel-like factor 2 (KLF2) and the pro-angiogenic cytokine IL-8. KLF2 has been shown to be involved in fluid shear stress, smooth muscle migration, and the regulation of endothelial cells, including negatively regulating inflammation and angiogenesis [18, 26–28]. KLF2 can repress both vascular endothelial growth factor (VEGF-A)-mediated angiogenesis, through down-regulation of VEGF receptor 2 (VEGFR2), as well as HIF1α expression and function [18, 27]. Following treatment by single-agent perifosine and the combination with rapamycin, KLF2 was markedly induced by 4.53- and 4.93-fold, respectively. IL-8 has previously been shown to be elevated in malignant renal cells compared to normal cells and may mediate resistance to the multi-kinase inhibitor sunitinib in advanced RCC [29–31]. Single-agent perifosine inhibited IL-8 expression by 2.3-fold, whereas the combination treatment down-regulated IL-8 by 2.7-fold. Single-agent rapamycin had no substantial effect on either KLF2 or IL-8 expression. We assessed the expression of both KLF2 and IL-8 by qRT–PCR to confirm the microarray data (Fig. 5a–c). At 24h post-treatment, an increase was observed in KLF2 expression of 6.5- and 6.9-fold in the perifosine alone and the combination arm, respectively, versus untreated controls. IL-8 showed a decrease in expression at 24h post-treatment of 2.6- and fivefold in the perifosine alone and the combination treatments. In each case, this differential expression was larger in the combination and was maintained through 72h after treatment. To test whether these effects were specific to 786-O, KLF2 and IL-8 expression was examined in the CAKI-1 cell line. As shown in Fig. 5e, KLF2 was induced beginning at 6h post-treatment with expression increasing to approximately 7.6-fold in the perifosine alone arm and 11.9-fold in the combination treatment after 24h of treatment. IL-8 expression showed no observable difference between any of the CAKI-1 treatment arms (data not shown). In the 786-O cells, we also analyzed the expression of the pro-angiogenic growth factor VEGF-A, which was observed on the microarray to be increased by 1.8-fold in the perifosine and combination treatments. Similar to those results, VEGF-A was induced beginning at 24h in both the perifosine and combination arms, by 2.3- and 1.52-fold, respectively (Fig. 5d). We also noted a subsequent increase at 72 h post-treatment in the levels of VEGF-A secreted into the media in the perifosine arm with only a small change in expression in the combination arm (Fig. 5f).

Gene ontology categories enriched following combination treatment

Gene Ontology (GO) analysis was performed to broadly identify biological processes that were altered following treatment by the combination of perifosine and rapamycin. GO categories that were enriched in the combination by five or more genes with differential expression of 2.00-fold or greater are shown in Online Resource 2. As indicated, most of the gene categories affected by the combination are not as well represented following single-agent treatment suggesting that there is an enhancement of drug activity when the agents are combined. Overall, the categories enriched by treatment include transcription, transport, metabolic processes (including proteolysis), cell cycling, apoptosis, and response to stress. Genes that were included in the analysis are listed by process in Online Resource 3. Gene Set Enrichment Analysis (GSEA) was also used to analyze the data set obtained from the treatment combination. Briefly, GSEA compares entire gene sets to each other in order to observe coordinated gene expression changes in different pathways where the effect on individual genes may be too low for our selection criteria. As shown in Online Resource 4, the combination induced changes in RCC-relevant gene sets including multiple gene sets relating to hypoxia/HIF1α status in endothelial cells, serum response in fibroblasts, and rapamycin or amino acid

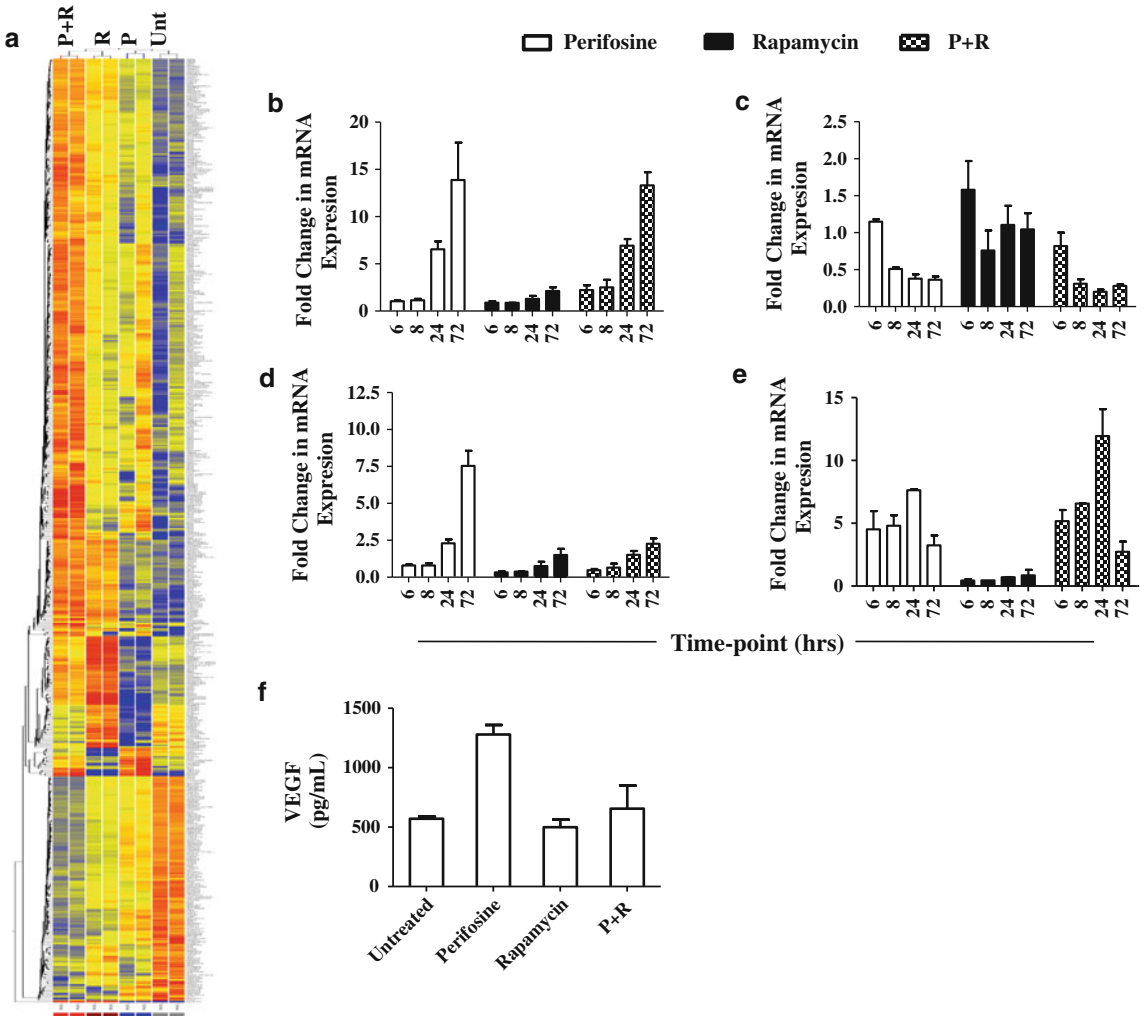

Fig. 5 Gene expression analysis using perifosine (5 mM), rapamycin (5 nM), and the combination compared to untreated. **a** Heat map of gene expression obtained from Affymetrix GeneChip microarray. Represents duplicates of perifosine (*P*), rapamycin (*R*), the combination ($P + R$), and untreated (*U*) 786-O cells following 24 h of treatment. qRT-PCR validation from 786-O cells of microarray data for (**b**) KLF2, (**c**) IL-8, and (**d**) VEGF following a time course. **e** qRT-PCR of treatment time course in CAKI-1 for KLF2. Fold change is relative to untreated. **f** Concentration of secreted VEGF-A following 72h of treatment

deprivation. Additional gene sets relating to vHL null and vHL wt status were both up-regulated following combination treatment suggesting a largely vHL-independent phenotype.

Discussion

The therapeutic landscape of advanced RCC is in rapid evolution. New systemic agents—particularly those targeting tumor angiogenesis and mTOR—have resulted in substantial improvements in response, progression-free survival, and in some cases, overall survival outcomes. In the United States, not less than six new agents have been approved by the Food and Drug Administration in the last 6 years for the treatment of advanced RCC. These include tyrosine kinase inhibitors (sunitinib, sorafenib, and pazopanib), VEGF-antibody-based therapy (bevacizumab in combination with interferon), and mTOR inhibitors (temsirolimus and everolimus). Unfortunately, none of these newer biologic therapies induce durable complete responses (a phenomenon which had been observed on occasion in patients treated with high-dose interleukin-2), nor have they cured a single patient with advanced RCC. Disease progression remains universal. Among the strategies proposed to overcome, these limitations has been combination therapy.

We pursued RCC preclinical modeling experiments that tested the concept of combined inhibition of the mTOR and Akt pathways, with the goal of achieving synergy and potentially overcoming Akt-mediated resistance to mTOR inhibition. In this study, we specifically examined the role

of perifosine, an orally bioavailable alkylphospholipid in the context of mTOR inhibition. While the precise mechanisms of action for perifosine are unknown, its known activities include inhibition of AKT activation through its interactions with lipid rafts in the plasma membrane [32, 33]. We found that although the addition of perifosine to rapamycin therapy did indeed result in the abrogation of rapamycin-induced Akt phosphorylation, there was no supra-additive or synergistic effect on growth inhibition or cytoxicity in in vitro conditions. However, by microarray analysis of the vHL-mutant (786-O) cell line, we observed an enrichment of genes having a 2-fold or greater change in expression in the combination versus single-agent treatment. Therefore, at least in terms of changes at the transcriptional level, the combination does produce some additive and supra-additive effects. And, while this does not appear to result in synergistic growth inhibition or cytotoxicity in cell line models, testing in an in vivo system may demonstrate treatment-induced activity on angiogenic and paracrine signaling.

As shown by the microarray analysis and confirmed by real-time PCR, perifosine as a single agent and in combination mediates the induction of KLF2, a repressor of HIF1alpha and a regulator of vascular endothelial quiescence. Additionally, we observed a concomitant reduction in the expression of the pro-angiogenic cytokine IL-8. This was coincident with a reduction in the protein level of HIF2alpha. However, we did identify an induction in both mRNA and secreted VEGF-A expression levels by 72 h post-treatment. While this effect was mitigated in the combination treatment arm, it suggests that perifosine may stimulate VEGF through a HIF-independent mechanism. Although VEGF has classically been described as being regulated by PI3K/AKT and HIF, Arany et al. have demonstrated that VEGF may be induced through coactivation of estrogen-related receptor alpha (ESRRA) and peroxisome proliferator-activated receptor gamma coactivator 1 alpha (PPARGC1A) following ischemia [34]. While it is unclear specifically what mechanism perifosine stimulates VEGF, alkylphospholipids have been shown to disrupt cellular homeostasis resulting in a wide-range of biologic effects. Among these effects include alterations in cholesterol transport and metabolism that lead to an accumulation of cholesterol in the cell which can disrupt multiple signaling pathways [32]. In the current analysis conducted on an in vitro monolayer, we are precluded from observing any effects related to vascular development and regulation that may result from the combination treatment. Given the often complex roles, both of these genes play with respect to the production of secreted ligands and growth factors and the consequences of such on angiogenesis and the tumor micro-environment further study with combined mTOR and AKT inhibition may be warranted.

In conclusion, the combination of the Akt inhibitor perifosine with the mTOR inhibitor rapamycin did meet the expected molecular consequences of pAKT abrogation but did not appear to result in enhanced cytotoxicity. However, significant effects were observed in gene expression, which may impact on production of angiogenic factors relevant for RCC growth, metastasis, and chemo-resistance. These results, relevant in the context of many active agents in the RCC therapeutic arena, emphasize the importance of performing preclinical mechanistic studies prior to the design, prioritization, and conduct of clinical trials that explore combination strategies.

Acknowledgment We greatly appreciate Ryan R. Davis (GER and Department of Pathology and Laboratory Medicine, UCD School of Medicine) for his expert technical assistance and consultation for the microarray experiments. The UC Davis Cancer Center Genomics and Expression Resource is supported by Cancer Center Support Grant P30 CA93373-01 (R.W.D.V.W.) from the NCI. We also appreciate funding from the Landgraf Family Fund and the Egan Family Fund.

References

1. Hudes G, Carducci M, Tomczak P, Dutcher J, Figlin R, Kapoor A, Staroslawska E, Sosman J, McDermott D, Bodrogi I, Kovacevic Z, Lesovoy V, Schmidt-Wolf IG, Barbarash O, Gokmen E, O'Toole T, Lustgarten S, Moore L, Motzer RJ (2007) Temsirolimus, interferon alfa, or both for advanced renal-cell carcinoma. N Engl J Med 356:2271–2281
2. Motzer RJ, Escudier B, Oudard S, Hutson TE, Porta C, Bracarda S, Grunwald V, Thompson JA, Figlin RA, Hollaender N, Urbanowitz G, Berg WJ, Kay A, Lebwohl D, Ravaud A (2008) Efficacy of everolimus in advanced renal cell carcinoma: a double-blind, randomised, placebo-controlled phase III trial. Lancet 372:449–456
3. Patel PH, Senico PL, Curiel RE, Motzer RJ (2009) Phase I study combining treatment with temsirolimus and sunitinib malate in patients with advanced renal cell carcinoma. Clin Genitourin Cancer 7:24–27
4. Hainsworth JD, Spigel DR, Burris HA, 3rd, Waterhouse D, Clark BL, Whorf R (2010) Phase II trial of bevacizumab and everolimus in patients with advanced renal cell carcinoma. J Clin Oncol 28:2131–2136
5. Escudier BJ, Negrier S, G. Gravis, C. Chevreau, R. Delva, J. Bay, L. Geoffrois, E. Legouffe, E. Blanc, C. Ferlay (2010) Can the combination of temsirolimus and bevacizumab improve the treatment of metastatic renal cell carcinoma (mRCC)? Results of the randomized TORAVA phase II trial. J Clin Oncol 28:15s (suppl; abstr 4516)
6. Wan X, Harkavy B, Shen N, Grohar P, Helman LJ (2007) Rapamycin induces feedback activation of Akt signaling through an IGF-1R-dependent mechanism. Oncogene 26:1932–1940
7. Chee KG, Longmate J, Quinn DI, Chatta G, Pinski J, Twardowski P, Pan CX, Cambio A, Evans CP, Gandara DR, Lara PN Jr (2007) The AKT inhibitor perifosine in biochemically recurrent prostate cancer: a phase II California/Pittsburgh cancer consortium trial. Clin Genitourin Cancer 5:433–437
8. Van Ummersen L, Binger K, Volkman J, Marnocha R, Tutsch K, Kolesar J, Arzoomanian R, Alberti D, Wilding G (2004) A phase I trial of perifosine (NSC 639966) on a loading dose/maintenance

dose schedule in patients with advanced cancer. Clin Cancer Res 10:7450–7456
9. Kondapaka SB, Singh SS, Dasmahapatra GP, Sausville EA, Roy KK (2003) Perifosine, a novel alkylphospholipid, inhibits protein kinase B activation. Mol Cancer Ther 2:1093–1103
10. Engel JB, Schonhals T, Hausler S, Krockenberger M, Schmidt M, Horn E, Koster F, Dietl J, Wischhusen J, Honig A (2011) Induction of programmed cell death by inhibition of AKT with the alkylphosphocholine perifosine in in vitro models of platinum sensitive and resistant ovarian cancers. Arch Gynecol Obstet 283:603–610
11. Purnell PR, Mack PC, Tepper CG, Evans CP, Green TP, Gumerlock PH, Lara PN, Gandara DR, Kung HJ, Gautschi O (2009) The Src inhibitor AZD0530 blocks invasion and may act as a radiosensitizer in lung cancer cells. J Thorac Oncol 4:448–454
12. Franken NA, Rodermond HM, Stap J, Haveman J, van Bree C (2006) Clonogenic assay of cells in vitro. Nat Protoc 1:2315–2319
13. Tepper CG, Vinall RL, Wee CB, Xue L, Shi XB, Burich R, Mack PC, de Vere White RW (2007) GCP-mediated growth inhibition and apoptosis of prostate cancer cells via androgen receptor-dependent and -independent mechanisms. Prostate 67:521–535
14. Tepper CG, Gregg JP, Shi XB, Vinall RL, Baron CA, Ryan PE, Desprez PY, Kung HJ, deVere White RW (2005) Profiling of gene expression changes caused by p53 gain-of-function mutant alleles in prostate cancer cells. Prostate 65:375–389
15. Irizarry RA, Hobbs B, Collin F, Beazer-Barclay YD, Antonellis KJ, Scherf U, Speed TP (2003) Exploration, normalization, and summaries of high density oligonucleotide array probe level data. Biostatistics 4:249–264
16. Subramanian A, Tamayo P, Mootha VK, Mukherjee S, Ebert BL, Gillette MA, Paulovich A, Pomeroy SL, Golub TR, Lander ES, Mesirov JP (2005) Gene set enrichment analysis: a knowledge-based approach for interpreting genome-wide expression profiles. Proc Natl Acad Sci USA 102:15545–15550
17. Boldrini L, Gisfredi S, Ursino S, Lucchi M, Mussi A, Basolo F, Pingitore R, Fontanini G (2005) Interleukin-8 in non-small cell lung carcinoma: relation with angiogenic pattern and p53 alterations. Lung Cancer 50:309–317
18. Kawanami D, Mahabeleshwar GH, Lin Z, Atkins GB, Hamik A, Haldar SM, Maemura K, Lamanna JC, Jain MK (2009) Kruppel-like factor 2 inhibits hypoxia-inducible factor 1alpha expression and function in the endothelium. J Biol Chem 284:20522–20530
19. Carroll VA, Ashcroft M (2006) Role of hypoxia-inducible factor (HIF)-1alpha versus HIF-2alpha in the regulation of HIF target genes in response to hypoxia, insulin-like growth factor-I, or loss of von Hippel-Lindau function: implications for targeting the HIF pathway. Cancer Res 66:6264–6270
20. Muller PY, Janovjak H, Miserez AR, Dobbie Z (2002) Processing of gene expression data generated by quantitative real-time RT-PCR. Biotechniques 32:1372–1374(1376), 1378–1379
21. Simon P (2003) Q-Gene: processing quantitative real-time RT-PCR data. Bioinformatics 19:1439–1440
22. Buck E, Eyzaguirre A, Brown E, Petti F, McCormack S, Haley JD, Iwata KK, Gibson NW, Griffin G (2006) Rapamycin synergizes with the epidermal growth factor receptor inhibitor erlotinib in non-small-cell lung, pancreatic, colon, and breast tumors. Mol Cancer Ther 5:2676–2684
23. Crul M, Rosing H, de Klerk GJ, Dubbelman R, Traiser M, Reichert S, Knebel NG, Schellens JH, Beijnen JH, ten Bokkel Huinink WW (2002) Phase I and pharmacological study of daily oral administration of perifosine (D-21266) in patients with advanced solid tumours. Eur J Cancer 38:1615–1621
24. Fu L, Kim YA, Wang X, Wu X, Yue P, Lonial S, Khuri FR, Sun SY (2009) Perifosine inhibits mammalian target of rapamycin signaling through facilitating degradation of major components in the mTOR axis and induces autophagy. Cancer Res 69:8967–8976
25. Chou TC, Talalay P (1984) Quantitative analysis of dose-effect relationships: the combined effects of multiple drugs or enzyme inhibitors. Adv Enzyme Regul 22:27–55
26. Wu J, Bohanan CS, Neumann JC, Lingrel JB (2008) KLF2 transcription factor modulates blood vessel maturation through smooth muscle cell migration. J Biol Chem 283:3942–3950
27. Sako K, Fukuhara S, Minami T, Hamakubo T, Song H, Kodama T, Fukamizu A, Gutkind JS, Koh GY, Mochizuki N (2009) Angiopoietin-1 induces Kruppel-like factor 2 expression through a phosphoinositide 3-kinase/AKT-dependent activation of myocyte enhancer factor 2. J Biol Chem 284:5592–5601
28. Lin Z, Kumar A, SenBanerjee S, Staniszewski K, Parmar K, Vaughan DE, Gimbrone MA Jr, Balasubramanian V, Garcia-Cardena G, Jain MK (2005) Kruppel-like factor 2 (KLF2) regulates endothelial thrombotic function. Circ Res 96:e48–e57
29. Fukata S, Inoue K, Kamada M, Kawada C, Furihata M, Ohtsuki Y, Shuin T (2005) Levels of angiogenesis and expression of angiogenesis-related genes are prognostic for organ-specific metastasis of renal cell carcinoma. Cancer 103:931–942
30. Konig B, Steinbach F, Janocha B, Drynda A, Stumm M, Philipp C, Allhoff EP, Konig W (1999) The differential expression of proinflammatory cytokines IL-6, IL-8 and TNF-alpha in renal cell carcinoma. Anticancer Res 19:1519–1524
31. Huang D, Ding Y, Zhou M, Rini BI, Petillo D, Qian CN, Kahnoski R, Futreal PA, Furge KA, Teh BT (2010) Interleukin-8 mediates resistance to antiangiogenic agent sunitinib in renal cell carcinoma. Cancer Res 70:1063–1071
32. Jimenez-Lopez JM, Rios-Marco P, Marco C, Segovia JL, Carrasco MP (2010) Alterations in the homeostasis of phospholipids and cholesterol by antitumor alkylphospholipids. Lipids Health Dis 9:33
33. van der Luit AH, Vink SR, Klarenbeek JB, Perrissoud D, Solary E, Verheij M, van Blitterswijk WJ (2007) A new class of anticancer alkylphospholipids uses lipid rafts as membrane gateways to induce apoptosis in lymphoma cells. Mol Cancer Ther 6:2337–2345
34. Arany Z, Foo SY, Ma Y, Ruas JL, Bommi-Reddy A, Girnun G, Cooper M, Laznik D, Chinsomboon J, Rangwala SM, Baek KH, Rosenzweig A, Spiegelman BM (2008) HIF-independent regulation of VEGF and angiogenesis by the transcriptional coactivator PGC-1alpha. Nature 451:1008–1012